

Charge transient spectroscopy

J. W. Farmer, C. D. Lamp, and J. M. Meese

University of Missouri, Research Reactor and University of Missouri–Columbia, Department of Physics, Columbia, Missouri 65211

(Received 22 July 1982; accepted for publication 14 September 1981)

A new variation of the deep level transient spectroscopy technique is presented. In the new approach, the current transient is integrated, yielding a charge transient. A simple circuit for integrating the current is given and is analyzed. The charge transient technique is compared to previous capacitance transient and current transient techniques, and the advantages of the new method are discussed. The effects of diode leakage currents are also analyzed. Data are presented for defects in neutron irradiated Si.

PACS numbers: 71.55.Fr, 61.80. — x

There are many variations of the original deep level transient spectroscopy (DLTS) technique.¹ Most of the previous methods have used either capacitance transients or current transients² to obtain information about deep levels in semiconductors. We present a novel approach in which current transients are integrated, yielding charge transients. The new technique will be referred to as charge transient spectroscopy (QTS). The QTS acronym will be used to avoid confusion with current transient spectroscopy. This new technique retains the high-speed advantages of a low impedance current amplifier often used in transient current spectroscopy, but overcomes the difficulty of loss of signal amplitude with decreasing thermal emission rate.

In the following we will discuss the basis of the QTS technique. The integration circuit is analyzed and the effects of leakage current are considered. The integration method makes possible the study of defects over a very wide range of time constants. The advantages of QTS compared to capacitance and/or current transient techniques are discussed. Finally, QTS data for neutron irradiated *n*-type Si are presented.

In the basic deep level transient spectroscopy technique, a reverse-biased diode is pulsed toward zero bias. The depletion width collapses and free carriers may become trapped at deep level defect sites. When the diode is returned to the initial reverse-bias condition, the trapped carriers will remain within the depletion width. As a function of time and temperature, the trapped charge will be thermally emitted and the junction will relax to its original state. The relaxation process is usually monitored by measuring either the junction capacitance or the junction current. **For the case of uniform trap distribution the current transient has the form^{2,3}**

$$i(t) = AqWN_T e^{-t/\tau} / 2\tau, \quad (1)$$

where A is the diode area, q is the elementary charge, W is the junction depletion width, N_T is the density of traps, and τ is the current-transient decay time constant. For majority-carrier traps in *n*-type material, τ is defined in terms of the carrier thermal emission rate e_n by the relationship

$$\tau^{-1} = e_n = N_c \sigma_n \langle v \rangle \exp[-(E_c - E_T)/kT], \quad (2)$$

where N_c is the effective density of states in the conduction band, σ_n is the carrier capture cross section, $\langle v \rangle$ is the carrier thermal velocity, $(E_c - E_T)$ is the trap depth below the con-

duction band, k is Boltzmann's constant, and T is the temperature.

In the QTS method, the current transient [Eq. (1)] is integrated electronically, i.e.,

$$q(t) = \int_0^t i(t') dt' = \frac{AqWN_T}{2} (1 - e^{-t/\tau}). \quad (3)$$

Note that the τ^{-1} prefactor found in Eq. (1) has been removed by the integration process. **The removal of the τ^{-1} prefactor gives the QTS method a significant advantage over current transient spectroscopy at large values of τ .**

The integration is performed by a very simple circuit. The circuit consists of a high-speed field-effect transistor operational amplifier (LF357) with no input resistor and with a parallel RC feedback loop. The circuit converts the current from the sample diode into a voltage. The form of the output of the circuit is found by considering the Laplace transforms of the input signal and the RC feedback loop.

The output voltage is given by

$$V(t) = \frac{AqWN_T R (e^{-t/RC} - e^{-t/\tau})}{2(RC - \tau)}.$$

For $RC \gg \tau$,

$$V(t) = (AqWN_T / 2C) [1 - e^{-t/\tau}]. \quad (4)$$

Comparison of Eq. (4) with Eq. (3) shows that $V(t) = q(t)/C$, thus the output of the circuit is directly proportional to $q(t)$, the integrated current, or transient charge.

There are two additional current signals which are also integrated by the present circuit. First, there are large current spikes associated with the voltage pulse applied to the sample diode. The integrator returns a voltage pulse with amplitude $\approx \Delta V \cdot C_d / C$, where ΔV is the voltage pulse applied to the diode and C_d is the diode capacitance. The integrated pulse may be several volts and in general must be suppressed to prevent the overloading of the analyzing circuits. A sample and hold amplifier (AD 583) was used to blank off the pulse in the present experiment. The second current is the reverse-bias leakage current of the sample diode. A constant leakage current i_l produces a dc offset $V_0 = i_l R$ which does not affect the QTS results. However, when the diode is pulsed to near zero volts, the leakage current drops to near zero. The result is a train of current pulses rather than a constant current i_l . Analysis of the integrator

output for a train of current pulses yields an output voltage signal due to leakage current of the form

$$V_l(t) = V_0 \left[1 - \left(\frac{1 - e^{-\beta \Delta t}}{1 - e^{-\beta P}} \right) e^{-\beta t} \right], \quad (5)$$

where $V_l(t)$ is the voltage output induced by the leakage current, $\beta = 1/RC$, t is the time after the bias pulse, Δt is bias pulse width, and P is the period of the pulse train.

In the case of a double boxcar measurement, the error due to a leakage current i_l is

$$\begin{aligned} E &= V_l(t_1) - V_l(t_2) \\ &= V_0 \left(\frac{1 - e^{-\beta \Delta t}}{1 - e^{-\beta P}} \right) [e^{-\beta t_1} - e^{-\beta t_2}]. \end{aligned} \quad (6)$$

For $\beta P \ll 1$, Eq. (6) reduces to

$$E = V_0 \beta \Delta t (t_1 - t_2) / P = i_l \Delta t (t_1 - t_2) / CP. \quad (7)$$

From Eq. (7) it is seen that the error is minimized by keeping Δt small and P large. The advantage of increasing P is obtained until $\beta P \approx 1$. At the limit $\beta P \gg 1$ (and $\beta \Delta t, \beta t_2 \ll 1$) the error is independent of P and is

$$E = (i_l \beta / C) (\Delta t) (t_1 - t_2).$$

There are three main advantages of the QTS technique. First is the simplicity of the measuring circuit. The simple integrating circuit replaces the role of a high-speed capacitance bridge for capacitance transient studies, and the role of a high-gain current amplifier for current transient studies. The second advantage is the very wide range over which τ can be measured with QTS. In principle, the upper limit of τ^{-1} that can be measured using the integrator is determined by the 20-MHz bandwidth of the LF357 operational amplifier. In the present configuration, the actual limit is determined by the bandpass of the sample and hold amplifier (1 MHz). The lower limit is determined by the requirement that $\tau \ll RC$. A practical upper limit for R is $10^{10} \Omega$. A value of $C = 20$ pF gives a very good signal amplitude and results in a $RC \approx 200$ ms.

If a larger RC is desired, the loss of signal associated with increasing C is readily offset by the addition of an oper-

ational amplifier gain stage after the integrator. A gain of 100 is easily attained. A third advantage is sensitivity. The sensitivity of the present configuration ($R = 10^9 \Omega$ and $C = 20$ pF) is estimated by comparing the noise level from an unirradiated diode with the predicted signal amplitude. Assuming a signal-to-noise ratio of 3, the minimum observable signal was found to be $5 \mu\text{V}$, or from Eq. (4), about 1200 traps. For our sample with $N_D = 10^{16} \text{ cm}^{-3}$, $A = 6.2 \times 10^{-4} \text{ cm}^2$ and $W = 1 \times 10^{-4} \text{ cm}$; 1200 traps correspond approximately to $N_T = 2.0 \times 10^{-6} N_D$. The technique is seen to be quite sensitive, especially compared to capacitance techniques. A current transient system with a carefully designed current amplifier has been reported with sensitivity of 900 traps as estimated from amplifier noise measurements with a capacitor used to simulate the sample.⁴ For a real diode sample with its additional shot noise, the sensitivities of this system and ours should be approximately the same.

A typical spectrum obtained from neutron irradiated n -type Si is shown in Fig. 1. The standard double boxcar technique was used. The gate times were 10 and 100 μs , which correspond to an $\tau_{\text{max}} = 3.9 \times 10^{-5} \text{ s}$. The integration time constant RC was 20 ms. At 300 K the leakage current is quite large ($\sim 10^{-8} \text{ A}$), however, the contribution of the leakage current to the difference signal $V(t_1) - V(t_2)$ is only 1.5% of the charge transient signal. The analysis of the QTS data is very similar to that of capacitance transient data. The peak signal corresponds to a relaxation time $\tau_{\text{max}} = (t_1 - t_2) / \ln(t_1/t_2)$. The number of defects can be determined by substituting τ_{max} into Eq. (4). Note that $S = [V(t_1) - V(t_2)] g$, where S is the signal amplitude of the boxcar output and g is the boxcar gain. For the data in Fig. 1, the numbers of defects are $E1 = 8.9 \times 10^{14} \text{ cm}^{-3}$, $E2 = 7.0 \times 10^{13} \text{ cm}^{-3}$, and $E3 = 9.3 \times 10^{14} \text{ cm}^{-3}$ ($N_D = 1.2 \times 10^{16} \text{ cm}^{-3}$).

An Arrhenius plot of a series of temperature scans is given in Fig. 2. Note that the τT^2 data span six decades. The

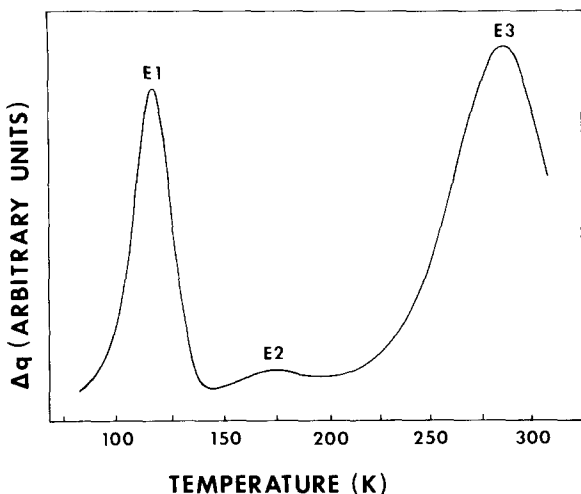


FIG. 1. QTS temperature scan for neutron irradiated n -type Si. $\tau_{\text{max}} = 3.91 \times 10^{-5} \text{ s}$.

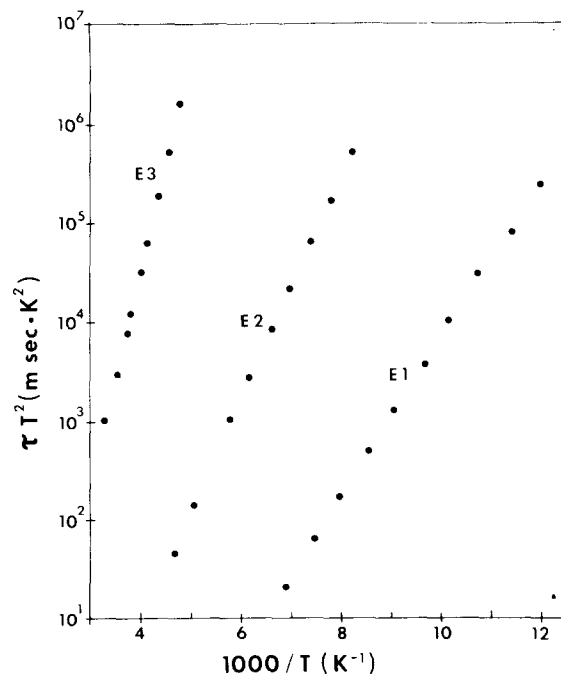


FIG. 2. Arrhenius plot of τT^2 vs $1/T$.

slopes and intercepts give

$$E_1 = 0.16 \text{ eV} \quad \sigma_1 = 3.5 \times 10^{-15} \text{ cm}^2$$

$$E_2 = 0.22 \text{ eV} \quad \sigma_2 = 8.8 \times 10^{-16} \text{ cm}^2$$

$$E_3 = 0.43 \text{ eV} \quad \sigma_3 = 4.9 \times 10^{-15} \text{ cm}^2.$$

These findings are in excellent agreement with results using capacitance transients,⁵ and are quite similar to capacitance results of electron irradiated Si.⁶

In conclusion, charge transient spectroscopy is a new variation of the basic DLTS technique. The heart of the method presented here is a simple circuit for integrating the current transient from the sample diode. This integration eliminates the τ^{-1} amplitude loss associated with current transient spectroscopy. The method is extremely fast, extending the range of measurements of τ over the previous

techniques by at least a factor of 10.^{1,2,4} The combination of the simplicity of the measurement technique, the wide range of τ that can be measured, and the good sensitivity makes QTS a very useful method for studying deep levels in semiconductors.

¹D. V. Lang, J. Appl. Phys. **45**, 3014 (1974); **45**, 3023 (1974).

²B. W. Wessels, J. Appl. Phys. **47**, 1131 (1976).

³C. T. Sah, L. Forbes, L. L. Rosier, and A. F. Tasch, Jr., Solid State Electron. **13**, 759 (1970).

⁴J. A. Borsuk and R. M. Swanson, IEEE Trans. Electron. Devices **ED-27**, 2217 (1980).

⁵J. W. Farmer and J. M. Meese, J. Nucl. Mater. (in press); J. M. Meese, M. Chandrasekhar, D. L. Cowan, S. L. Chang, H. Yousif, H. R. Chandrasekhar, and P. McGrail, in *Neutron Transmutation Doped Silicon*, edited by J. Guldborg (Plenum, New York, 1981), p. 101.

⁶L. C. Kimerling, IEEE Trans. Nucl. Sci. **NS-23**, 1497 (1976).

High-field electron transport in $\text{In}_x\text{Ga}_{1-x}\text{As}_y\text{P}_{1-y}$ ($\lambda_g = 1.2 \mu\text{m}$)

T. H. Windhorn, L. W. Cook, and G. E. Stillman

Electrical Engineering Research Laboratory,^{a)} Materials Research Laboratory, and Coordinated Science Laboratory, University of Illinois at Urbana-Champaign, Urbana, Illinois 61801

(Received 9 August 1982; accepted for publication 14 September 1982)

A fixed-frequency microwave time-of-flight technique has been used to measure electron drift velocities in $\text{In}_x\text{Ga}_{1-x}\text{As}_y\text{P}_{1-y}$ ($\lambda_g = 1.2 \mu\text{m}$) at temperatures 95–400 K and electric field strengths of up to 200 kV/cm. The room-temperature electron drift velocity in the quaternary is equal to the velocity in GaAs for field strengths greater than ~ 62 kV/cm, but the velocity is higher in the quaternary for field strengths from about 20–62 kV/cm at 300 K. At temperatures above 300 K the high-field velocity is larger in the quaternary than in GaAs, but below 300 K the high-field velocity is larger in GaAs.

PACS numbers: 72.20.Ht, 72.80.Ey

There has been widespread interest in $\text{In}_x\text{Ga}_{1-x}\text{As}_y\text{P}_{1-y}$, grown lattice matched to InP, during the past several years because of the potential for application of these alloys to both optoelectronic and microwave devices. A variety of optoelectronic devices has been fabricated from various compositions of this quaternary alloy, but reports of efforts to construct and characterize microwave devices from these materials have been rather limited.^{1,2} High values of the low-field mobility and peak electron drift velocity are desirable for low noise, high-frequency devices. The low-field mobilities have been extensively studied,^{3–9} and the peak velocities and threshold fields^{3,9,10} have been measured over a wide compositional range. A knowledge of the drift velocity at fields beyond threshold is also important, however, if predictions about the efficiencies of transferred electron oscillators are to be made. Transferred electron oscillation has been reported for one composition ($E_g = 1.05$ eV, $T = 300$ K) of the quaternary,¹ but no attempt was made to optimize the efficiency (0.5% at 27.49 GHz). In this letter we report the first measurements of electron drift velocities in

$\text{In}_x\text{Ga}_{1-x}\text{As}_y\text{P}_{1-y}$ ($\lambda_g = 1.2 \mu\text{m}$) at fields beyond threshold. Drift velocities were measured using a fixed-frequency (7.54 GHz) microwave time-of-flight technique.¹¹ A detailed description of the experimental apparatus used for these measurements is presented elsewhere.¹²

The $\text{In}_x\text{Ga}_{1-x}\text{As}_y\text{P}_{1-y}$ samples used in the measurements were grown by liquid phase epitaxy on Sn-doped (100) InP substrates. After the growth of an n^+ -InP buffer layer, a lightly doped n -type quaternary layer and finally a thin (~ 4000 Å) Zn-doped ($\sim 1.0 \times 10^{17} \text{ cm}^{-3}$) layer were grown forming a pn homojunction near the surface. The thickness and net electron concentration of the n -type quaternary layer were determined from capacitance-voltage measurements at 1 MHz. Sixteen devices taken from four different wafers were used for the measurements. The n -type quaternary layers ranged in thickness from 5.2 to 15 μm . The doping profiles for several typical layers are shown in Fig. 1. The band gap and amount of lattice mismatch were determined using optical transmission and x-ray diffraction techniques, respectively. The room-temperature band gap in the quaternary material was 1.03 eV ($\lambda_g = 1.2 \mu\text{m}$), and the lattice mismatch between the quaternary and the InP was always

^{a)}Department of Electrical Engineering.